

Research article

Solution Combustion Synthesis and Characterization of Nano crystalline Lanthanum Ferrite using Glycine as a fuel

G. Venkaiah, K. Venkateswara Rao*, V. Sessa Sai Kumar, CH. Shilpa Chakra

Centre for Nano Science and Technology, Institute of Science and Technology,

Jawaharlal Nehru Technological University Hyderabad, Hyderabad-500 085.

Corresponding author Email: kalagadda2003@gmail.com

Abstract

In this paper we discuss about the synthesis of the nano sized crystalline Lanthanum Ferrite (LaFeO_3) by solution combustion synthesis where lanthanum nitrate, iron nitrate were taken as metal precursors and glycine was taken as fuel. The ratio of fuel to oxidizer was taken as one ($\psi = 1$). The prepared nanocrystalline LaFeO_3 were characterized by X-ray diffraction, Thermo gravimetric and differential thermal analysis, Nano particle size analyzer, UV-Visible absorption spectrometer, Scanning Electron Microscopy with Energy Dispersive X-ray Analysis spectrum (EDAX) and the investigation of magnetic properties showed in hysteresis curve used VSM. **Copyright © IJMMT, all rights reserved.**

Keywords: Solution Combustion Synthesis, nanocrystalline LaFeO_3 , X-ray diffraction, Scanning Electron Microscopy, FTIR, UV-Vis Spectrometer and vibration sample magnetometer.

1. Introduction

Physical and chemical properties of LaBO_3 (B=transition metal) perovskite oxides have been widely studied as they have well-defined structure and high thermal stability. LaBO_3 with a typical ABO_3 -type crystals can have broad applications in advanced technologies such as solid oxide fuel cells, catalysts and chemical sensors, magnetic materials, electrode materials, etc.[1-3]. LaFeO_3 oxide is a weak ferromagnetic material with interesting magnetic and magneto-optical properties [4-5]. In the present generation it is promising for various technological, industrial and research fields for the development of different applications [6]. Various studies are made on the photo catalytic activity of Lanthanum Ferrite (LFO) and hence they have drawn conclusions that LFO exhibits different properties like high stability, non-toxicity and small band gap energy depending on their size [7-10].

Solution combustion synthesis (SCS) is a simple, suitable and fast process for synthesizing the variety of Nano size materials in the range (1-100 nm). This process involves initial medium is aqueous solution of different oxidizers (e.g., metal nitrates) and fuels (e.g. glycine, urea, Hexa methylene tetra amine (HMTA), hydrazides). This process depends on the volume or layer-by-layer self-propagating combustion modes. This process is not only for synthesizing nano sized oxide materials but also allows standardized doping of suggestive amounts of rare-earth contamination ions in a single step. Using solution combustion method various possible oxides structures could be prepared such as perovskite (e.g. LaFeO_3), spinel (e.g. MgAl_2O_4), garnet (e.g. $\text{Y}_3\text{Fe}_5\text{O}_{12}$), hexa ferrite (e.g. $\text{SrFe}_{12}\text{O}_{19}$) etc. The latest developments in SCS technique have paved way for the several materials applications [11-12].

2. Experimental and Characterization Details

2.1 Preparation of Nano crystalline Lanthanum Ferrite powder

Lanthanum ferrite nanopowdered sample was prepared by solution combustion synthesis method, in which different precursors are used in stoichiometric amounts of taken as ratios. Fuel (organic compound) and Oxidizer (metal nitrates) compositions were calculated using reducing valences of fuel compounds and of oxidizing valences of metal nitrates. The materials are La (NO₃)₃•6H₂O, Fe (NO₃)₃•9H₂O and glycine mixed in 1:3 ratio and added to 40 ml distilled water in a beaker. The ratio of the fuel to oxidizers is taken as one (ψ =1).The entire mixture were mixed on a magnetic stirrer up to 20 min. It formed completely aqueous solution, after that the mixture of solution is placed on hot plate. The temperature slowly increases to eliminate the water from clear solution. During this process we observed boiling, frothing, fumes, smoldering and flaming. After flaming if finally forms nanocrystallite LaFeO₃ powder.

The balanced equation is as follows



2.2 Characterization Techniques

The crystallite size and structural characterization obtained from BrukerD8 Advanced X-ray diffractometry using a Cu K α radiation $\lambda=1.5409 \text{ \AA}$ and (h k l) values corresponding with JCPDF card No: 75-0145 calculated from Debye-Scherrer's equation. Thermo gravimetric and Differential thermal analyzer (Model NO: A 6300R) using to study the thermal stability of the sample. Approximately 7 mg of the sample were heated at the rate 20 ° C /min up to 800 °C. Band gap energy and absorption peak at particular wavelength study using for Systronics UV-Vis Spectrometer 2202. SEM micrographs obtained from a HITACHI S3400N scanning electron microscope, coupled with energy dispersive X-ray spectrometer using for elements percentage in sample. Particle size analyzer (HORIBA NANO PARTICLE ANALYZER SZ-100) observed the sample have narrow size nanoparticles calculated with from Debye-Scherrer's equation. Magnetic properties was investigated in VSM.

3. Results and Discussion

3.1 Structural Analysis

The crystal structure and crystallite size of the sample were characterized by X-ray diffraction. The XRD patterns were collected from BrukerD8 Advanced X-ray diffractometry using a Cu K α radiation $\lambda=1.5409 \text{ \AA}$ and the crystallite size is calculated equation at particular peaks low and high intensity were range (20 ° ≤ 2 θ ≤ 80°) as shown in fig (1). The crystallite size range from 14nm-30nm to be found the average crystallite size of LaFeO₃ is 25 nm using the Debye-Scherrer equation [1] is

$$D = \frac{K\lambda}{\beta \cos \theta} \dots \dots \dots (1)$$

Where K is constant its value 0.9, λ is the x-ray wavelength, θ is the Bragg's angle and β is the full width half maxima at reflecting intensity peaks. And this crystallite powder size is 27±0.00189 nm and lattice distortion 0.000875±0.00218 is obtained from the graph $\beta \cos \theta$ vs. $2 \sin \theta$ at extrapolation and slope using Williamson-Hall equation [2] is

$$\beta \cos \theta = \frac{K\lambda}{t} + 2\epsilon \sin \theta \dots \dots \dots (2)$$

Here β is the full width at half maxima in radians and θ is the Bragg's angle in radians.

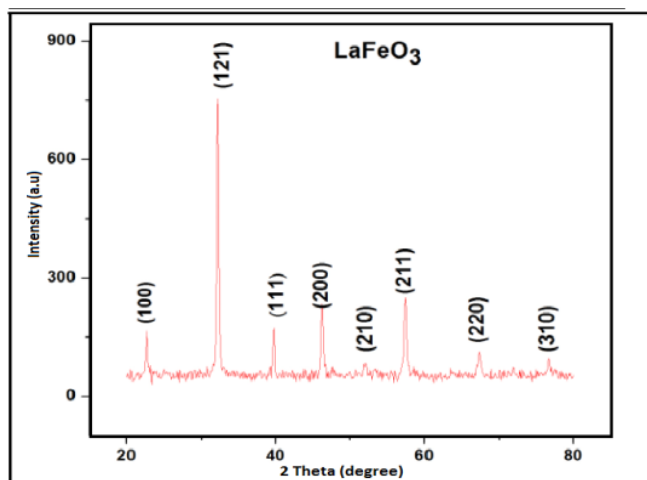


Figure 1: .XRD pattern of LaFeO₃ nano powder

3.2 Thermo Gravimetric and Differential Thermal Analysis

Thermo gravimetric and differential thermal analysis was performed to study the thermal analysis behavior of the nano crystalline powder and respective curves as shown in below fig (2). This sample decomposition starts with increase in temperature; at below 100⁰C adsorbed water evaporated from the sample, hence weight loss is 0.15% is observed. The small amount of weight loss is point to noble environment and transparent size lanthanum ferrite formed for the period of calcination. The final weight loss is 2.82% obtained in TG curve from fig 2(a), using the temperature range is less than 800⁰C.

In the fig 2(b) DTA curve the starting step of the sample decomposition to remove adsorption and chemisorbed water in designated by endothermic peak is observed 58⁰C and exothermic peak was observed at 311⁰C here temperature 100⁰C-800⁰C in DTA curve

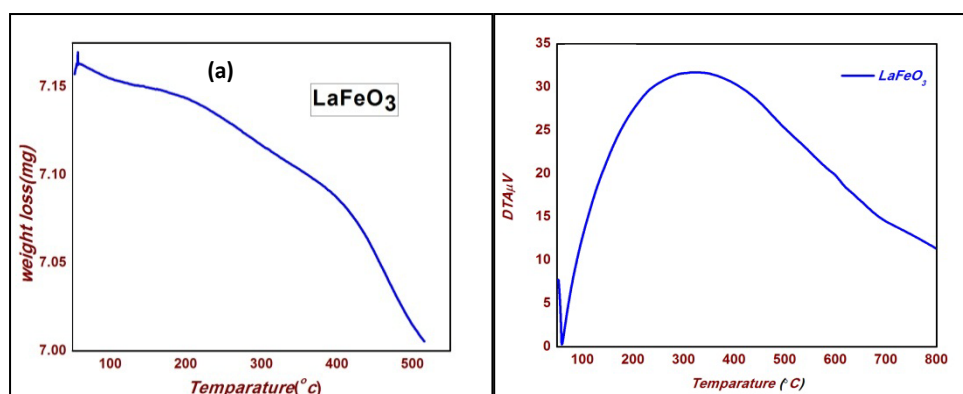


Figure 2: (a) TG curve with temperature (b) DTA curve with temperate of synthesized LaFeO₃ nanopowders.

3.3 UV-Vis Spectroscopy

LFO crystallite size powders were well dispersed in distilled water to form a colloidal mixture by subjecting to ultra – sonication for 15min. After sonication using this solution placed in UV –Vis spectrometer, after 2min we observed absorption broad peak at 350nm in the fig 4(a) and the band gap energy is 2.46eV obtained from the

graph as shown in Fig 4(b) using extrapolation at αhv is zero, the absorption coefficient for direct band gap LFO using Tauc relation equation [3] is

$$(\alpha hv) = A(hv - E_g)^{1/2} \dots\dots\dots (3)$$

Here $h\nu$ is photon energy, E_g is the energy band gap of sample, A is the constant which is different for different transitions.

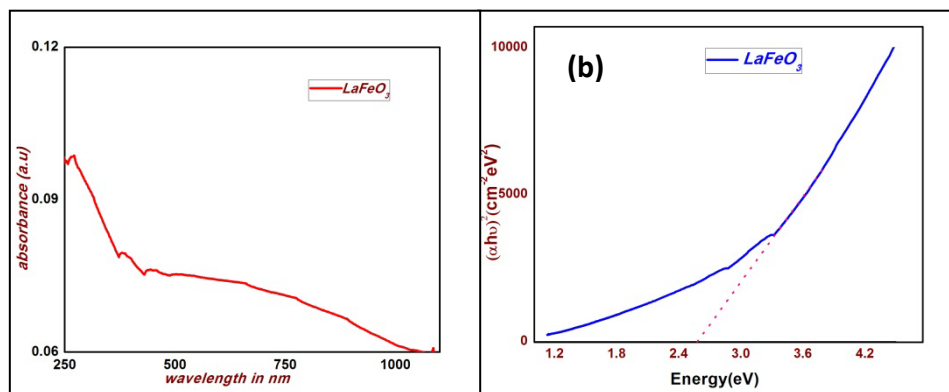


Figure 3: shows (a) Absorption of LFO nanopowder with wavelength in nm and (b) shows band gap by extrapolation of (αhv) Vs $h\nu$ of LFO nanopowder

3.4 FTIR Spectrum Analysis

The LFO nanopowders were mixed with appropriate amount KBr salts to form pellets in order to observe FTIR spectra. FTIR spectra with wavenumber ranges from 450-4000 cm^{-1} is as shown in fig (4) for LFO nanopowder. We observed five sharp peaks in figure at 3465 cm^{-1} due to the stretching vibrations of hydroxyl group (ν_{O-H}), 1641 cm^{-1} is due to asymmetric carbonyl group ($\nu_{C=O}$), 1556 cm^{-1} and 1454 cm^{-1} both are symmetric stretched bands of COO^- , 545 cm^{-1} around the peak corresponds to Fe-O stretching vibration mode [16-18].

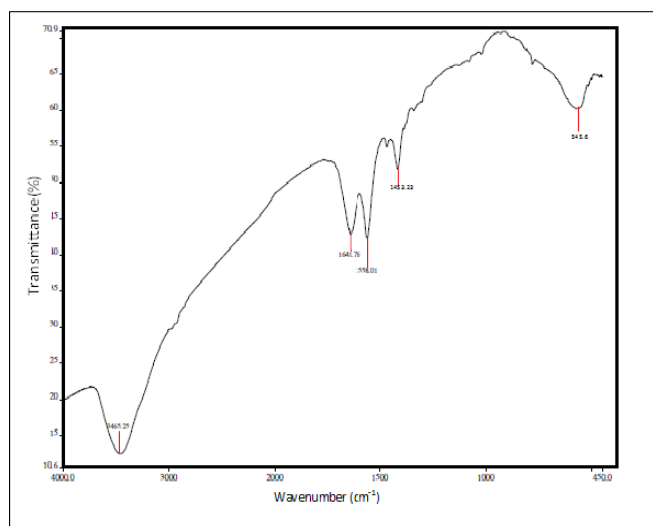


Figure 4: FTIR spectrum of LFO Nano crystals

3.5 SEM and EDAX analysis

The SEM equipment was employed to result surface topography of LFO. The particle shape is not cleared in the image, as shown in fig (5) many large pores in the entire material. We assumed that the pores are mostly

intergranular. The chemicals in LFO particles are investigated with EDAX magnification are 10 μ m which confirmed atomic ratio of LFO (La, Fe) is 1:1 and there is no another elements are not identified.

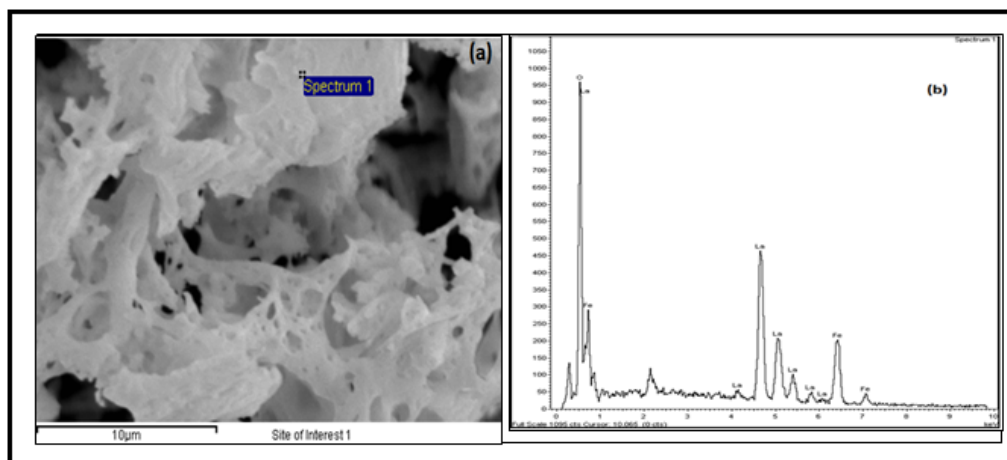


Figure 5: (a)SEM image with EDS at particular area of spectrum (b) LFO contain shows La, Fe.

Element	Weight %	Atomic %
O K	34.33	76.78
Fe K	16.45	10.54
La L	49.22	12.68
Totals	100	100

Table1: shows composition of elements in LFO using EDAX

3.6 Particle Analysis

The particle narrow size distribution obtained by particle size analyzer using dynamic light scattering technique (HORIBA SZ-100 DLS with input energy 532nm).It was clearly observed in Fig (6). That LFO nanoparticles average particle size is 31nm dispersed within the range of about 14-30nm which is well matched with XRD reflected peaks calculated by Debye-Scherrer equation.

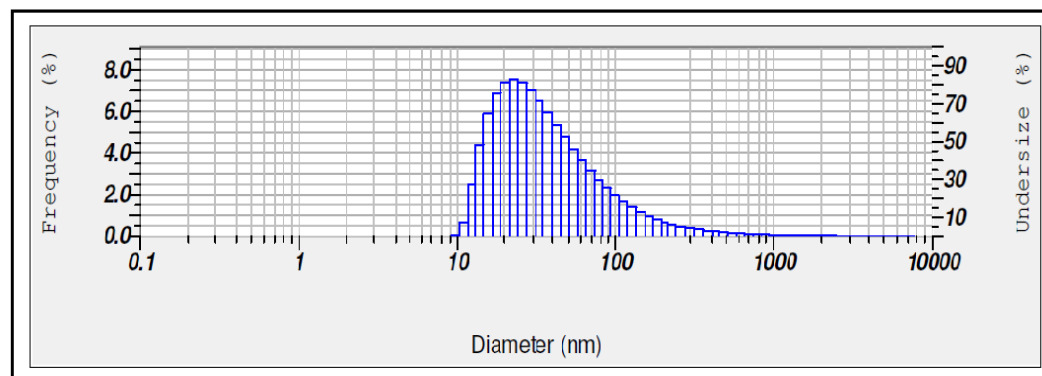


Figure 6: Particle Analysis of LFO nanopowder

3.7 Magnetic properties of LFO nano-sized powder

The magnetic properties of LaFeO₃ nano-sized powder was investigated, as shown in Fig. 7. The calcined at 350°C nanocrystalline LaFeO₃ powder show antiferromagnetic behavior, with obvious hysteresis loop. The calcined LaFeO₃ exhibits much smaller retentivity magnetization 0.175emu/g and smaller coercivity 184Oe. The combustion process involves a rapid exothermic redox reaction between the metal nitrates and an appropriate fuel. During the process, the crystalline structure of LaFeO₃ is considerably deformed, resulting in observed magnetization. When the powder is calcined, the deformation of the structure is released. LaFeO₃ is known to be antiferromagnetic produce as weak ferromagnetism [19]. The net magnetization of LaFeO₃ very small because of the antiferromagnetic order of the Fe³⁺ spins. Only a slight canting of the adjacent Fe³⁺ spins produces weak ferromagnetism. The spontaneous magnetization is observed to be 6.581 emu/g and magnetic moment as 0.286 emu/mole of LaFeO₃ nanopowder compared with bulk crystals at room temperature [20].

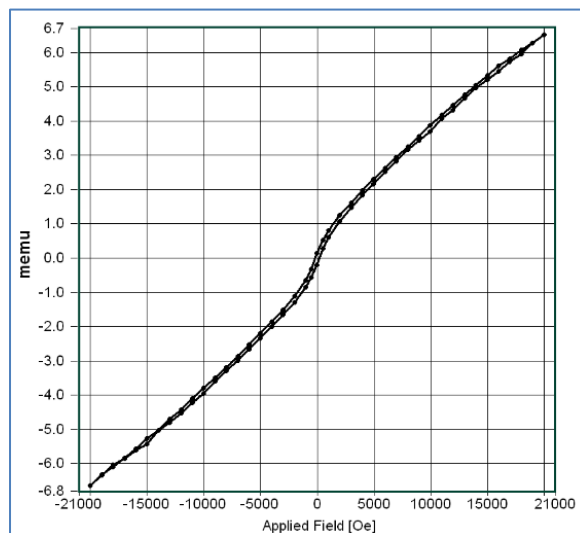


Figure 7: Hysteresis loop of LaFeO₃ nanopowder at room temperature.

Conclusions

In the present investigation, LFO nanopowder was prepared with glycine as a fuel by Solution Combustion Synthesis and average crystallite size is observed to be 25nm calculated using Debye-scherrer equation. XRD results confirmed the crystallite size of LFO nanopowders is 27 nm which is in good agreement with particle size as 31nm obtained by particles size analyzer. UV Vis spectroscopy revealed absorption and the energy band gap as 273 nm and 2.46eV respectively. At low energy band gap it is suitable for photo catalytic applications. TG/DTA curves showed the 2% weight loss from the sample. Exothermic and endothermic peaks are observed at 58°C and 311°C respectively. Fe-O stretching vibration mode band is observed at wavenumber 545 cm⁻¹ from FTIR analysis. It was observed many pores in SEM analysis. The LaFeO₃ nanoparticles exhibited weak-ferromagnetism behavior and had anomalous small magnetization.

References

- [1] F. J. Berry, X. Ren, J. R. Gancedo, Jose F. Marco, *Hyperfinem Interact*, 156., 2004, 335
- [2] Q. Zhang, F.Saito, *Journal of Material Science*, 36., 2001. 2287
- [3] S. Nakayama, *Journal of Material Science*, 36., 2001, 5643
- [4] D. Treves, *Journal of Applied Physics*, 36, 1965, 1033-1039
- [5] Y.S. Didosyan, H. Hauser, H. Wolfmayr, *Sens.Actuators A* 106, 2003, 168-171
- [6] Huang K, Lee H Y and Goodenough J B *Journal of the Electrochemical Society*, 45, 1998, 3220
- [7] Wang Y, Yang X, Lu L, Wang X. *ThermochimActa*, 443, 2006, 225-30
- [8] Li S, Jing L, Fu W, Yang L, Xin B, Fu H. *Mater Res Bull*, 42,2007, 203-12

- [9] Hoffman MR, Martin ST, Choi W, Chemical Reviews, 95., 1995, 69-96
- [10] M. Siva Kumar, A. Gedanken, W. Zhong, Journal of material chemistry, 14., 2004, 764 –769
- [11] Singanahally T. Aruna, Alexander S. Mukasyan. Solid State Material Science, 12., 2008, 44–50
- [12] Kashinath C. Patil, S.T. Aruna, TanuMimani. Solid State Material Science, 6., 2002, 507–512
- [13] A.R.West, Solid state chemical and its applications, John Wiley & Sons, London, 1984, 174
- [14] H. Kameli, H. Salamati, and A. Aezami, Journal of Applied Physics, 2006
- [15] Tauc J (Ed.) Amorphous and Liquid Semiconductor, Plenum press, New York. (1974).
- [16] Xiangting Dong, Jinxian Wang, Qizheng Cui, International Journal of Chemistry, vol. 1, Feb. 2009, No.1
- [17] Manjunath B Bellakki Bull. Material Science, Vol.33, No. 5, Octo. 2010, 611–618
- [18] T. Baraniraj, P. Philominathan, Journal of Minerals and Materials Characterization and Engineering, Vol.10, 2011. No.4
- [19] Treves D Studies on Orthoferrites at the Weizmann Institute of Science. , Journal of Applied Physics, 36, 1965, 1033-1039
- [20] Shen H, Cheng G, Wu A, Xu J, Zhao J Combustion synthesis and characterization of nano-crystalline LaFeO₃ powder. Physica Status Solidi (a), 206., 2009, 1420-1424